

Photoconductive organic materials for the near-IR radiation range

N. A. Davidenko,^{a*} N. A. Derevyanko,^b A. A. Ishchenko,^b N. G. Kuvshinsky,^a
A. V. Kulinich,^b O. Ya. Neiland,^{†c} and M. V. Plotniece^c

^aTaras Shevchenko Kiev National University,
64 ul. Vladimirska, 01033 Kiev, Ukraine.
E-mail: daviden@ukrpack.net

^bInstitute of Organic Chemistry, National Academy of Sciences of Ukraine,
5 ul. Murmanska, 02094 Kiev, Ukraine.

Fax: +10 380 (44) 573 2643. E-mail: alexish@i.com.ua

^cRiga Technical University,
14 ul. Azenes, LV-1048 Riga, Latvia.
Fax: (371) 761 5972

Polymer composition films based on polystyrene and containing electron donors, viz., substituted tetrathiafulvalenes, an electron acceptor, viz., 2,4,5,7-tetranitrofluoren-9-one, and sensitizers, viz., a cationic polymethine dye, 1,3,3-trimethyl-2-[3-(1,3-dihydro-1,3,3-trimethyl-2*H*-indol-2-ylidene)prop-1-en-1-yl]-3*H*-indolium tetrafluoroborate, and a neutral mero-cyanine dye, 5-{3-[(1,3-dihydro-1,3,3-trimethyl-2*H*-indol-2-ylidene)ethylidene]-2-phenylcyclopent-1-en-1-ylmethylene}-2-thioxodihydropyrimidine-4,6(1*H*,5*H*)-dione, were prepared. The internal photoeffect upon film irradiation in the near-IR range is provided by low ionization potentials of the donors and the high electron affinity of the acceptor. The photoconductivity increases upon replacement of a cationic dye by a neutral one, mainly because of photogeneration of mobile charge carriers of both signs and a decrease in the activation energy for the photoconduction current. The decrease in the activation energy for the photocurrent is due to the fact that in the case of a neutral dye, the mobile charge carriers move away from each other during their separation, while in the case of a cationic dye, the colorless counterion strongly holds the photogenerated charge carrier.

Key words: electron–hole pairs, organic dyes, photogeneration of charge carriers, polymer compositions, tetrathiafulvalenes.

The design of the materials that conduct electric current on exposure to near-IR radiation is a fairly topical task for photoelectric solar energy converters.^{1–3} Along with inorganic semiconductors, the use of organic polymers and their compositions for this purpose appears promising.^{1,4–6} These are selected or developed with allowance for the requirements to their films placed between the electrical contacts in the sandwich structures of photoelectric converters.⁷ Generally, the photoconductivity of polymer films is provided by the presence of three types of molecules: donors, acceptors, and photogeneration centers of charge carriers.⁸ If the donor molecules are characterized by the ionization potential $E_{i,d}$ (proportional to the HOMO energy) and the acceptor molecules, by the electron affinity $A_{e,a}$ (proportional to the LUMO energy),⁹ the molecules of the photogeneration centers are selected to meet the conditions $|E_{i,c}| > |E_{i,d}|$ and $|A_{e,c}| < |A_{e,a}|$, where $E_{i,c}$ and $A_{e,c}$ are the ionization

potential and the electron affinity of the photogeneration center molecule, respectively. If these conditions are fulfilled, the absorption of a light quantum gives an electron–hole pair (EHP). Dissociation of the EHP results in free charge carriers.

An important condition for the photoconduction is the transport of charge carriers within the bulk of the polymer film toward the electrical contacts without capture or recombination.^{10–15} These structural features and properties of polymeric materials have already been implemented in films based on carbazolyl-containing polymers and polymers with conjugated bonds,⁵ which use either intermolecular charge transfer complexes (CTC) or organic dyes and their aggregates as IR absorption and charge carrier photogeneration centers.

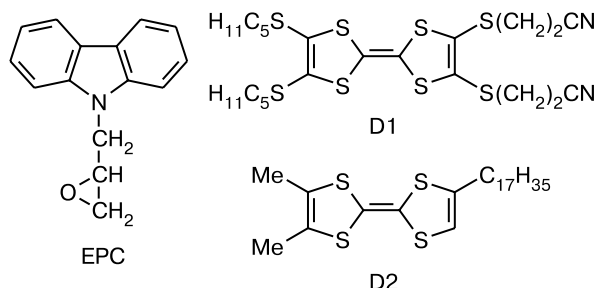
However, known polymeric compositions exhibit only low conductivity on exposure to near-IR radiation due to high $|E_{i,d}|$ values of the donor molecules and/or low $|A_{e,a}|$ values of the acceptor molecules with respect to the molecules of photogeneration centers, whose $|E_{i,c}| - |A_{e,c}|$

[†] Deceased.

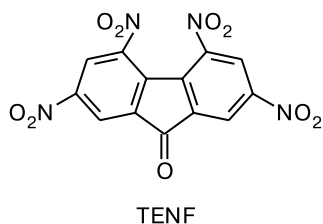
energy difference should be as low as possible. In addition, dissociation of the EHP is affected appreciably by the electronic structure of the donor and acceptor molecules, in particular, the more pronounced delocalization of the frontier MO, the weaker the Coulomb attraction between the charge carriers in the EHP and the higher the probability of their separation.¹⁶ Therefore, it would be desirable to use strong organic donors and acceptors, for example, tetrathiafulvalenes and fullerenes.^{17,18} The drawbacks of these compounds include poor solubility in and poor compatibility with polymer binders and also the difficulty of preparing polymers containing these compounds.

The purpose of this work is to study the photophysical properties of films formed from polymer compositions with various organic donors, acceptors, and photogeneration centers represented by ionic and neutral dyes. The solution of this problem is expected to provide the key to the creation of new effective photoconductive materials for the near-IR region of the spectrum.

Polystyrene (PS) was used as the polymer base and epoxypropylcarbazole (EPC) and tetrathiafulvalenes D1 and D2 were employed as the donor molecules. They are readily soluble in nonpolar solvents and are less prone to aggregation in the polymeric binder than similar tetrathiafulvalenes without aliphatic tails.

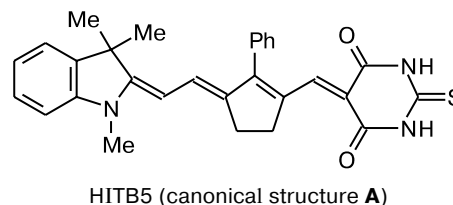
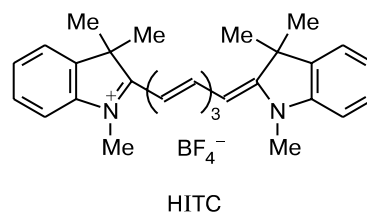


2,4,5,7-Tetranitrofluoren-9-one (TENF) functioned as the acceptor.

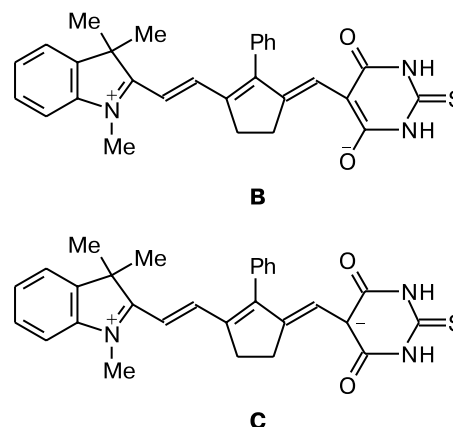


Either the CTC formed by EPC, D1, or D2 with TENF or the dyes HITC and HITB5 acted as the photogeneration centers.

In carbazoyl-containing polymer films, cationic polymethine dyes, in particular HITC, behave as hole photogeneration centers.¹⁹ The merocyanine dye HITB5 exhibits positive photochromism. Thus, its ground state is mainly described by the neutral canonical structure **A**,



while the excited state is described by a set of bipolar structures of types **B** and **C**.



Therefore, these merocyanines can be regarded as photogeneration centers of both holes and electrons. Particular attention should be placed on the extensive color and the high absorption intensity of the specially synthesized merocyanine HITB5, which is unusual for this type of dyes. The point is that merocyanines, which are electron-asymmetric dyes, contain alternating single and double bonds in the polymethine chain,²⁰ unlike symmetrical polymethines, for example, HITC in which these bonds are largely equalized.²¹ This bond alternation, similarly to that in polyenes, induces a hypochromic and hypsochromic effects in the absorption spectra. Therefore, the absorption bands of merocyanines are located at shorter wavelengths than these bands for the corresponding symmetrical (parent) dyes with the same length of the polymethine chain.^{20,21} As the chain length increases, the degree of alternation is enhanced, resulting in attenuation of the vinylene shifts in merocyanines, as opposed to symmetrical cyanines.^{22,23} The merocyanine HITB5 we synthesized absorbs virtually in the same region as the cationic dye HITC. This substantial color deepening was attained by introducing five-membered rings into the even positions of the chromophore, resulting in a bathochromic

shift of bands and a hyperchromic effect,²² and by using the thiobarbituric acid residue with a greater effective length of the chromophore as the terminal group.^{22,24}

Experimental

Compounds EPC,²⁵ D2,²⁶ and HITC²⁷ were prepared by known procedures. Compound D1 was mentioned in a previous study;²⁸ however, its synthesis was not reported. ¹H NMR spectra were measured on a Varian spectrometer (400 MHz).

4',5'-Bis(cyanoethylthio)-4,5-bis(pentylthio)-2,2'-bis-1,3-dithiole (D1). A suspension of 4,5-bis(cyanoethylthio)-1,3-dithiol-2-one²⁸ (1.16 g, 4.02 mmol) and 4,5-bis(pentylthio)-1,3-dithiol-2-thione²⁶ (1.56 g, 4.02 mmol) was refluxed for 1.5 h at 120 °C in freshly distilled triethylphosphite under argon. After 110 min, the suspension turned into a dark-brown solution and after an additional 20 min, a precipitate formed. The reaction mixture was cooled to ~20 °C and diluted with 10 mL of MeOH. The precipitate was filtered off and dried in air. The product was chromatographed on SiO₂ (Silica Gel Grade 62, 60–200 mesh, Aldrich; elution with CH₂Cl₂) to collect the middle fraction with *R_f* 0.7. After concentration of the eluate, the residue was crystallized from a CH₂Cl₂–MeOH mixture (1 : 3). Yield 1.4 g (61%), m.p. 92–94 °C (*cf.* Ref. 28: m.p. 93–94 °C, yield 64%). ¹H NMR (CDCl₃), δ: 0.85 (t, 6 H, 2 Me, *J* = 6.0 Hz); 1.50–1.70 (m, 12 H, 6 CH₂); 2.70 (t, 4 H, SCH₂CH₂CN, *J* = 6.0 Hz); 2.80 (t, 4 H, SCH₂R, *J* = 6.0 Hz); 3.05 (t, 4 H, CH₂CN, *J* = 6.0 Hz).

5-{3-[(1,3,3-Trimethyl-1,3-dihydro-2*H*-indol-2-yliden)ethyliden]-2-phenylcyclopent-1-en-1-ylmethylene}-2-thioxodihydropyrimidine-4,6(1*H*,5*H*)-dione (HITB5). A mixture of 1,3,3-trimethyl-2-[(*E*)-2-[3-[(*E*)-*N*-acetyl-*N*-phenylamino-methylidene]-2-phenylcyclopent-1-yl]ethen-1-yl]-3*H*-indolium tetrafluoroborate (0.272 g, 0.5 mmol)²² and thiobarbituric acid (0.072 g, 0.5 mmol) in 5 mL of 95% EtOH was heated to boiling for 1 h in the presence of 0.5 mL of Et₃N. After cooling, the precipitate that formed was filtered off and washed with small amounts of EtOH and Et₂O. Yield 0.116 g (48%), dec.p. 249–250 °C (from AcOH). UV/Vis (CH₂Cl₂), λ_{max}/nm (ε/L mol^{–1} cm^{–1}): 741 (219600). UV/Vis (DMF), λ_{max}/nm (ε/L mol^{–1} cm^{–1}): 745 (181000). Found (%): C, 72.03; H, 5.44; N, 8.86. C₂₉H₂₇N₃O₃S. Calculated (%): C, 72.32; H, 5.65; N, 8.72. ¹H NMR (DMSO-*d*₆), δ: 1.339 (s, 6 H, Me₂C); 2.859, 3.207 (both t, 2 H each, CH₂CH₂, *J* = 6.3 Hz); 3.412 (s, 3 H, NMe); 5.699 (d, 1 H, NC=CH, *J* = 13.2 Hz); 6.989 (t, 1 H, H(5)_{indole}, *J* = 7.6 Hz); 7.048 (d, 1 H, H(7)_{indole}, *J* = 7.6 Hz); 7.073 (d, 1 H, NC=CH–CH, *J* = 13.2 Hz); 7.18–7.30 (m, 4 H, H arom.); 7.512 (s, 1 H, CH=CCO); 7.52–7.60 (m, 3 H, H arom.); 11.486 (s, 2 H, NH).

Quantum-chemical calculations for the compounds under study were carried out by semiempirical AM1 method with a standard set of parameters.²⁹ The calculation included the interaction of singly excited configurations caused by all the possible electron transitions from the three upper HOMO to the three lower LUMO. The molecular geometry was first optimized using the restricted Hartree–Fock calculation and the Polack–Ribiere algorithm with an accuracy of 0.001 kcal Å^{–1} mol^{–1}.

The samples with the free surface of the polymer film of the sandwich structures with the SnO₂–In₂O₃ and Al contacts were prepared by a known procedure.¹³ The concentration of the

donor molecules with respect to the PS weight varied from 0 to 30%, that of TENF, from 0 to 20%, and that of the dye, from 0 to 1%. For the sample with the free film surface, the spectra of the absorption coefficient (κ/κ₄₀₀) of the polymer film were measured, where κ₄₀₀ is the absorption coefficient at λ = 400 nm. In the sandwich samples, the dark current (*j_d*) and photocurrent (*j_{ph}*) densities under irradiation with monochromatic light were measured. The light intensity (*I*) in the range of 0.2–5.0 W m^{–2} was varied by neutral light filters. The electric field intensity (*E*) in the polymer film varied in the range of (1–20) · 10⁷ W m^{–1}. The current kinetics with time during the irradiation and after switching off the light was recorded using a storage oscilloscope. The *j_d* and *j_{ph}* values were measured in the temperature range (*T*) from 290 to 355 K. The dependences of *j_d* and *j_{ph}* on *T* were used to determine the activation energies of the electrical conductivity (*W_i*) and photoconductivity (*W_{ph}*), respectively.

Results and Discussion

The PS films containing no additives do not absorb visible light in the region of λ > 400 nm, while in sandwich structures, they do not display the photoconductivity effect over the whole range of *E*. If the films contain the acceptor TENF, the long-wavelength edge of the proper absorption of TENF becomes visible in the PS spectrum at λ > 400 nm (Fig. 1, curve 1). The PS + EPC (1–30% (w/w)) films containing no additives do not absorb light in the visible region and do not exhibit photoconductivity in the sandwich samples. The PS + D1 (1–30% (w/w)) and PS + D2 (1–30% (w/w)) films absorb at λ > 400 nm, due to the edge of proper absorption of D1 and D2 (see Fig. 1, curves 2 and 3). As the concentration of the donors increases, κ increases proportionally, but the shape of the absorption bands does not change. This attests to low tendency of EPC, D1, and D2 molecules for aggregation in the PS films. However, the optical absorption spectra of the PS + EPC, D1, D2 (1–30% (w/w)) + TENF (1–20% (w/w)) films contain new broad absorption bands absent from the spectra of the above-mentioned films (see Fig. 1, curves 4–6). As the TENF concentration increases, κ for the visible and near-IR ranges increases, but the shape of the absorption bands does not change. This indicates that the absorption bands are due to the formation of CTC between the donors EPC, D1, and D2 and the acceptor TENF. The bathochromic shift of the long-wavelength absorption edge for the films upon the replacement of EPC by D1 or D2 is dictated by the decrease in *E_{i,d}* in this sequence of donors and the decrease in the light quantum energy (*hν_{ct}*) needed for complete electron transfer from the donor to the acceptor in the CTC³⁰

$$h\nu_{ct} = E_{i,d} - A_{e,a} - Q, \quad (1)$$

where *Q* is the interaction energy between the separated charges in the CTC. This is confirmed by comparison of

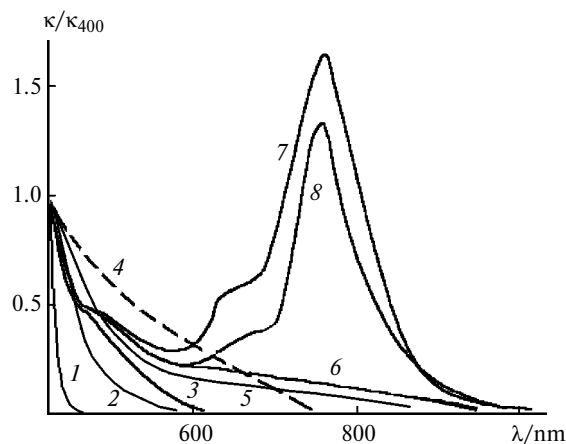


Fig. 1. Spectra of the absorption coefficient (κ/κ_{400}) of the films: PS + TENF (10% (w/w)) (1), PS + D1 (20% (w/w)) (2), PS + D2 (20% (w/w)) (3), PS + EPC (20% (w/w)) + TENF (10% (w/w)) (4), PS + D1 (20% (w/w)) + TENF (10% (w/w)) (5), PS + D2 (20% (w/w)) + TENF (10% (w/w)) (6), PS + D2 (20% (w/w)) + TENF (10% (w/w)) + HITC (1% (w/w)) (7), and PS + D2 (20% (w/w)) + TENF (10% (w/w)) + HITB5 (1% (w/w)) (8). κ_{400} is the absorption coefficient at $\lambda = 400$ nm.

the experimental $E_{i,d}$ values for EPC, D1, and D2 and by the results of quantum-chemical calculations of the HOMO and LUMO energies. The $|E_{i,d}|$ value for carbazole is 7.6 eV, according to the photoelectron spectroscopy data,²⁵ while for D1 and D2, these values are 6.7–6.9 and 6.25 eV, respectively, as estimated from the absorption spectra with various acceptors.²⁶ The results of our quantum-chemical calculation of the HOMO and LUMO energies for the donor, the acceptor, and the dyes used are shown in Fig. 2. Note that the results of these calculations are inapplicable for highly accurate numerical determination of the ionization potentials and the electron affinities of molecules. However, one can draw quite reliable qualitative conclusion on whether or not relation (1) holds upon replacement of the dopants in the PS films. It can be seen that the $|E_{i,d}|$ value decreases in the series EPC, D1, D2.

The sandwich samples with the PS + EPC, D1, D2 (1–30% (w/w)) + TENF (1–20% (w/w)) films were found to exhibit photocurrent in the absorption regions corresponding to the CTC (bathochromic shift upon the replacement of EPC by D1 and D2). When the E and I are constant, the j_{ph} value increases with an increase in the donor and/or acceptor concentration and does not depend on the polarity of the electric voltage applied, but decreases with an increase in λ in proportion to the change of κ . In addition, the dependences of j_{ph} on I are straight lines, while the dependences of j_{ph} on E can be approximated by straight lines in the $\log j_{ph}$ vs. $E^{1/2}$ coordinates (Fig. 3). From the slope ratio of these straight lines, one can calculate the Pool–Frenkel constant, and the result-

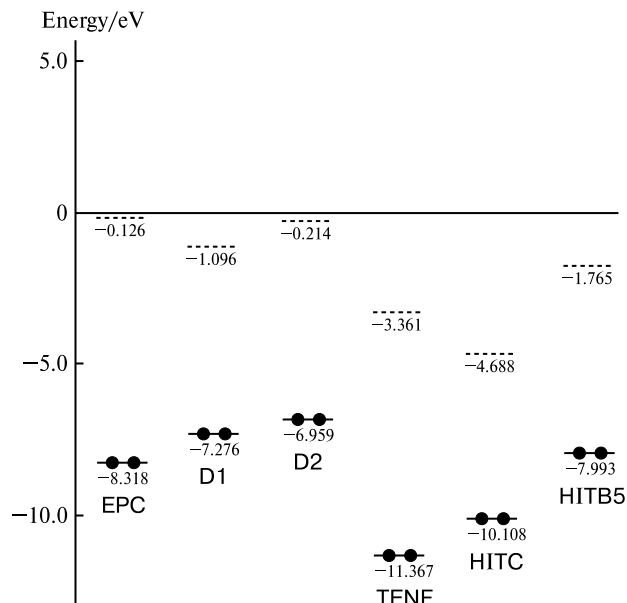


Fig. 2. HOMO (continuous horizontal lines) and LUMO (dashed horizontal lines) energies of the molecules under consideration.

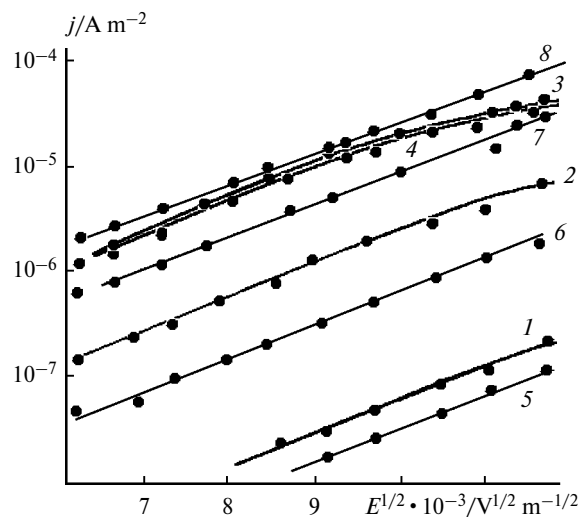


Fig. 3. Dark current (1–4) and photocurrent (5–8) densities (j) vs. electric field intensity (E) in the sandwich samples with the films: PS + EPC (20% (w/w)) + TENF (10% (w/w)) + HITB5 (1% (w/w)) (1, 5), PS + D1 (20% (w/w)) + TENF (10% (w/w)) + HITC (1% (w/w)) (2, 6), PS + D2 (20% (w/w)) + TENF (10% (w/w)) + HITC (1% (w/w)) (3, 7), and PS + D2 (20% (w/w)) + TENF (10% (w/w)) + HITB5 (1% (w/w)) (4, 8); $\lambda = 760$ nm, $T = 293$ K.

ing value, equal to $4.5 \cdot 10^{-5} \text{ eV V}^{-1/2} \text{ m}^{-1/2}$, is close to the theoretical one.^{8,17} The dark current and the photocurrent increase with an increase in the temperature. This implies that the photoconductivity of the samples is due to the bulk photogeneration of charge carriers and their transport in the polymeric films, the mechanism of carrier

photogeneration being similar to that accepted for poly-*N*-epoxypropylcarbazole films with TENF.^{8,17} CTC are the photogeneration centers in the EHP; the dissociation of the EHP in an external electric field occurs through the intermolecular transfer of holes over the donor molecules (EPC, D1, D2) and the transfer of electrons over the acceptor molecules (TENF).

In the sandwich samples with films containing donors, TENF, and dyes, both the dark current and the photocurrent are much higher than those in similar samples without the dyes (see Fig. 3). However, the samples with the PS + EPC (1–30% (w/w)) + TENF (1–20% (w/w)) + HITC, HITB5 (1% (w/w)) films develop a relatively low photocurrent in the dye absorption range ($\lambda > 700$ nm), which increases as EPC is replaced by D1 or D2. In addition, the photocurrent observed in the absorption range of the dye increases upon the replacement of HITC by HITB5, although the absorption coefficient in the case of HITB5 is lower than for HITC (see Fig. 1). The dark current and the photocurrent do not depend on the polarity of the electric voltage applied. The highest rate of the building-up and relaxation of the photocurrent, which characterizes the velocity of non-equilibrium charge carriers in an electric field,⁸ is found for samples with the films containing D2, TENF, and HITB5 (Fig. 4). The dependences of j_t and j_{ph} on T are linear in the Arrhenius coordinates, and the calculated

activation energies W_t and W_{ph} are close to each other. For example, the W_t and W_{ph} values found for the sandwich samples with the PS + D2 (20 % (w/w)) + TENF (10% (w/w)) + HITB5 (1% (w/w)) films at low E are equal to 0.23 ± 0.01 eV, while those for the samples with the PS + D2 (20% (w/w)) + TENF (10% (w/w)) + HITC (1% (w/w)) films are 0.45 ± 0.02 eV. This means that the photoconductivity and the electrical conductivity in these films at $\lambda > 700$ nm are mainly due to the bulk generation of charge carriers from the dye molecules. The HITB5 and HITC molecules serve as the photogeneration centers for nonequilibrium charge carriers and the centers of thermofield charge carrier generation.

An increase in the electrical conductivity and photoconductivity in the polymeric films containing EPC, D1, D2, and HITC indicates that the energy difference $|E_{i,c}| - |E_{i,d}|$ increases for this series of donors and the conditions for the formation of mobile charge carriers (holes) improve. It can be seen from Fig. 2 that the necessary condition of hole formation from excited dye molecules, $|E_{i,c}| > |E_{i,d}|$, holds for HITC and HITB5 with the donors we used, while the condition of electron generation, $|A_{e,c}| < |A_{e,a}|$, holds only for HITB5 with the TENF acceptor. This means that, unlike HITC, the HITB5 molecules can function as photogeneration centers for not only holes but also electrons. This can be confirmed experimentally, because the photocurrent in the PS films with D1 and D2 containing HITB5 and TENF (see Fig. 4, curve 6) is much higher than the sum of the photocurrents in similar samples containing either HITB5 or TENF, all other factors being the same. The photocurrent in the samples with PS films with D1 and D2 containing HITC and TENF is close to the sum of photocurrents in analogous samples containing either HITC or TENF (see Fig. 4).

However, an increase in the photoconductivity of films with HITB5 with respect to analogous films containing HITC has one more reason, in particular, the replacement of HITB5 by HITC results in higher W_t and W_{ph} . Within the model that implies two-step photogeneration of the carriers *via* the formation and dissociation of EHP, the W_{ph} value calculated from the plots for the variation of j_{ph} vs. T at low E values can be identified with the energy of Coulomb interaction between the electron and the hole in the EHP

$$W_{ph}^0 = q^2/4\pi\epsilon_0\epsilon r_0, \quad (2)$$

where q is the electron charge, ϵ_0 is the dielectric constant, ϵ is the dielectric permittivity, r_0 is the distance between the oppositely charged carriers in the EHP. The nonexcited dye molecules can be represented in the simplified form as (D—A) for HITB5 and (D—D⁺...An[−]) for HITC, where An is the colorless counterion of the ionic dye. The formation of the EHP in the PS films with D2,

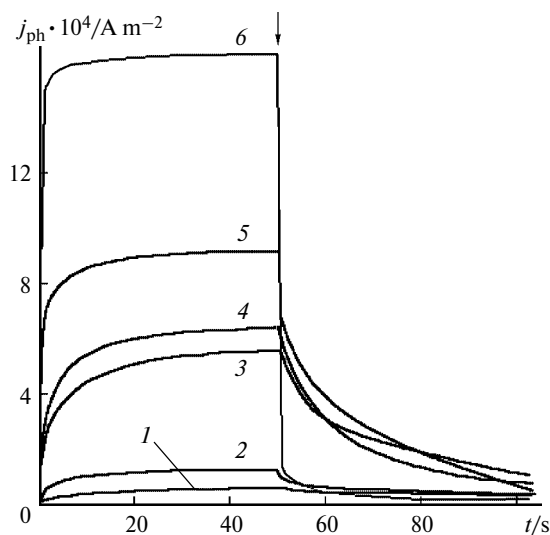
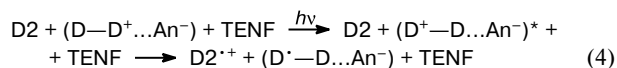
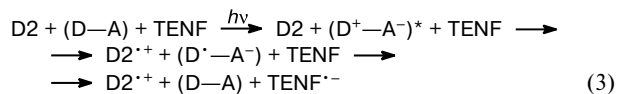


Fig. 4. Photocurrent density (j_{ph}) vs. time (t) of the irradiation with light with $\lambda = 760$ nm in sandwich samples with the films: PS + D1 (20% (w/w)) + TENF (10% (w/w)) (1), PS + D2 (20% (w/w)) + TENF (10% (w/w)) (2), PS + D2 (20% (w/w)) + HITC (1% (w/w)) (3), PS + D2 (20% (w/w)) + TENF (10% (w/w)) + HITC (1% (w/w)) (4), PS + D2 (20% (w/w)) + HITB5 (1% (w/w)) (5), and PS + D2 (20% (w/w)) + TENF (10% (w/w)) + HITB5 (1% (w/w)) (6). The vertical arrow shows the instant the light is switched off ($E = 1.1 \cdot 10^8$ V m^{−1}, $I = 1$ W m^{−2}, $T = 293$ K, polymer film thickness 1.5 μ m).

TENF, and HITB5 or with D2, TENF, and HITC can be represented by the following reactions with electron transfer.



Here, we took into account the fact that immediately after absorption of the light quantum, redistribution of the electron density takes place within the dye molecules to give their excited states, $(\text{D}^+-\text{A}^-)^*$ for HITB5 and $(\text{D}^+-\text{D}\dots\text{An}^-)^*$ for HITC. The relaxation of the excited states of the photogeneration centers gives rise to charge carriers. In the samples with PS films containing D2, TENF, and HITB5, the excited state of the dye molecule gives rise to a hole, represented by the D2 radical cation ($\text{D2}^{*\cdot+}$) and the HITB5 radical anion ($\text{D}^{\cdot}-\text{A}^-$), which can further give off the electron to the TENF molecule to yield the radical anion ($\text{TENF}^{\cdot-}$). In the samples with PS films containing D2, TENF, and HITC, absorption of light by the cationic dye molecule gives only a hole ($\text{D2}^{*\cdot+}$) and a radical anion contact pair ($\text{D}^{\cdot}-\text{D}\dots\text{An}^-$) consisting of a neutral radical and the counterion.

Equations (3) and (4) show the major difference between neutral and ionic dyes as regards photogeneration of charge carriers. This difference is in the fact that reactions (3) afford electrically charged radical ion pairs, which provide transport of the carriers, and electrically neutral molecules of photogeneration centers, whereas reactions (4) give electrically charged radical ion pairs to transport the carriers and the colorless counter-ions of the photogeneration centers. Since in the second photogeneration step, *i.e.*, dissociation of charge pairs, the mobile charge carriers move away from the oppositely charged centers, it can be stated that the activation energy of photogeneration W_{ph}^0 in the films with ionic dyes, unlike the films with neutral dyes, is determined by the energy of Coulomb interaction between the mobile charge carrier and the electrically charged colorless counterion; in this case, the r_0 value in Eq. (2) corresponds to the distance from the photogenerated carrier to this counterion.

Our assumption concerning the difference between the neutral and ionic dyes as photogeneration centers provides an interpretation for the increase in W_{ph}^0 upon the replacement of HITB5 by HITC. This interpretation is as follows. In the PS films with donors, acceptors, and HITB5, the spatial distribution of the dopant molecules is isotropic and no admixed ions are present. Therefore, during photogeneration of charge carriers from the HITB5 molecules, any direction of the radius-vector between the charges in the EHP can be considered to be equally probable for each particular molecule of the photogeneration

center. In the PS films with donors, acceptors, and HITC, the spatial distribution of the dopant molecules is also isotropic but they contain colorless ions whose concentration is equal to that of the photogeneration centers. The molecules of ionic organic dyes in the PS films may occur both as separated and contact charge pairs. This means that during the EHP formation, the outflow of the charge carriers from $(\text{D}^+-\text{D}\dots\text{An}^-)^*$ onto the donor molecules would be mainly directed toward the nearest An^- counterion. In this case, the distance r_0 should be shorter and the energy of the Coulomb interaction between the opposite charges should be higher. Note also that, since the electric charge in the colorless counterion of the ionic dye is highly localized, this energy increases to even a greater extent compared to that involved in the formation of EHP by reaction (3).¹⁶ The thermal generation of charge carriers from dye molecules also yields pairs of opposite charges and, therefore, the W_i and W_{ph} values are close to each other, but they are different for different types of dyes.

Tetrathiafulvalenes can be used as electron donors to produce polymer films that exhibit photoconductivity on exposure to near-IR radiation. For increasing their solubility and decreasing the aggregation, which results in a higher electric conductivity of polymeric compositions, the donor molecules must be provided with bulky substituents, for example, aliphatic radicals (D1 and D2 molecules). Aggregation can also be prevented by their cross-linking to the polymeric chain. Organic dyes should be used preferably as the photogeneration centers of charge carriers in the IR region of the spectrum. It should be borne in mind that the use of cationic dyes in polymeric films with a high concentration of the donors results in a monopolar photoconductivity, due to more efficient photogeneration of the holes. The less mobile electrons that remain in the cationic dye molecules after photogeneration of the EHP are efficient capture and recombination centers for charge carriers. In the films with ionic dyes, which function as photogeneration centers for charge carriers, the electric charge of the colorless counterions influences the photogeneration of the mobile charge carriers. At the first step of photogeneration, the photogenerated carriers are concentrated near these counterions. The electrostatic interaction in these charge pairs determines the activation energy for the photogeneration and the electrical conductivity. Since the distances between the charges in these pairs can be short, the experimental results obtained previously on the influence of the counterion type on the spin effects of the photoconductivity³¹ and recombination luminescence³² become interpretable. The photogeneration of charge carriers of both signs is ensured in the polymer films containing donors, acceptors, and neutral dyes. High photoconductivity is attained due to the fact that both the holes and the electrons are mobile in EHP photogeneration and their recombination in the dye molecule is hampered. In these films with

neutral dyes, photogeneration of the mobile charge carrier takes place in the electrostatic field of the ionized photogeneration center and, hence, the spatial distribution of the radius-vector between the charges in the EHP appears isotropic, and the energy of electrostatic interaction between the charges in the EHP can be lower than that in the case of ionic dyes, all other factors being the same.

References

1. N. C. Greenham, P. Xiaogang, and A. P. Alivisatos, *Phys. Rev. B*, 1996, **54**, 17628.
2. J. Rostalski and D. Meissner, *Solar Energy Mater., Solar Cells*, 2000, **61**, 87.
3. A. Ishchenko, N. Derevyanko, Yu. P. Piryatinskii, A. Verbitsky, D. Filonenko, and S. Studzinsky, *Mater. Sci.*, 2002, **20**, 5.
4. N. N. Barashkov, M. E. Globus, A. A. Ishchenko, I. P. Krainov, T. M. Murav'eva, V. V. Pomerantsev, V. V. Popov, O. K. Rossikhina, V. G. Senchishin, and A. V. Sidel'nikova, *Zhurn. Prikl. Spektrosk.*, 1991, **55**, 906 [*J. Appl. Spectr.*, 1991, **55** (Engl. Transl.)].
5. J.-M. Nunzi, *C. R. Physique*, 2002, **3**, 1.
6. W. U. Huynh, J. J. Dittmer, and A. P. Alivisatos, *Science*, 2002, **295**, 2425.
7. N. A. Davidenko, and A. A. Ishchenko, *Teoret. Eksperim. Khim.*, 2002, **38**, 84 [*Theor. Exp. Chem.*, 2002, **38**, 88 (Engl. Transl.)].
8. N. G. Kuvshinskii, N. A. Davidenko, and V. M. Komko, *Fizika amorfnykh molekulyarnykh poluprovodnikov [The Physics of Amorphous Molecular Semiconductors]*, Lybid', Kiev, 1994, 174 pp. (in Russian).
9. D. Danovich, Y. Apeloig, and S. Shaik, *J. Chem. Soc., Perkin Trans. 2*, 1993, 321.
10. E. L. Frankevich, A. N. Chaban, and D. I. Kadyrov, *Khim. Fiz.*, 2002, **21**, 103.
11. R. F. Khairutdinov, *Usp. Khim.*, 1998, **67**, 125 [*Russ. Chem. Rev.*, 1998, **67** (Engl. Transl.)].
12. N. F. Uvarov and V. V. Boldyrev, *Usp. Khim.*, 2001, **70**, 307 [*Russ. Chem. Rev.*, 2001, **70** (Engl. Transl.)].
13. N. A. Davidenko and A. A. Ishchenko, *Fizika Tverdogo Tela*, 2000, **42**, 1365 [*Phys. Sol. State*, 2000, **42** (Engl. Transl.)].
14. N. A. Davidenko and A. A. Ishchenko, *Pis'ma v Zhurn. Tekhn. Fiz.*, 2002, **28**, 84 [*JTP Lett.*, 2002, **28**, 483 (Engl. Transl.)].
15. N. Derevyanko, A. Ishchenko, and A. Verbitsky, *Mater. Sci.*, 2002, **20**, 13.
16. N. G. Kuvshinsky, N. A. Davidenko, V. V. Reshetnyak, L. I. Savransky, and V. L. Sheptun, *Chem. Phys. Lett.*, 1990, **165**, 323.
17. M. Pope and C. E. Swenberg, *Electronic Processes in Organic Crystals*, Clarendon Press, Oxford, 1982, 712 pp.
18. N. O. Mchedlov-Petrosyan, V. K. Klochkov, G. V. Andrievsky, and A. A. Ishchenko, *Chem. Phys. Lett.*, 2001, **341**, 237.
19. N. Davidenko, A. Ishchenko, N. Derevyanko, and V. Pavlov, *Mol. Cryst. Liq. Cryst.*, 2001, **361**, 71.
20. I. Baraldi, G. Brancolini, F. Momicchioli, G. Ponterini, and D. Vanossi, *Chem. Phys.*, 2003, **288**, 309.
21. A. A. Ishchenko, *Stroenie i spektral'no-lyuminescentnye svoistva polimetinovykh krasitelei [Structure and Spectral-Luminescence Properties of Polymethine Dyes]*, Naukova dumka, Kiev, 1994, 232 pp. (in Russian).
22. A. I. Tolmachev, Yu. L. Slominskii, and A. A. Ishchenko, *New Cyanine Dyes Absorbing in the NIR Region*, in *NATO ASI (Ser. 3)*, Kluwer Academic Publ., Dordrecht—Boston—London, 1998, **52**, 385.
23. A. A. Ishchenko, *Izv. Akad. Nauk. Ser. Khim.*, 1994, 1227 [*Russ. Chem. Bull.*, 1994, **43**, 1161 (Engl. Transl.)].
24. A. A. Ishchenko, *Izv. Akad. Nauk, Ser. Khim.*, 1996, 2194 [*Russ. Chem. Bull.*, 1996, **45**, 2079 (Engl. Transl.)].
25. V. D. Filimonov and E. E. Sirotkina, *Khimiya monomerov na osnove karbazola [Chemistry of Carbazole-Based Monomers]*, Nauka, Novosibirsk, 1995, 533 pp. (in Russian).
26. Ya. N. Kreitsberga, D. V. Bite, V. E. Kampar, R. B. Kampare, and O. Ya. Neiland, *Zhurn. Organ. Khim.*, 1981, **17**, 1055 [*J. Org. Chem. USSR*, 1981, **17** (Engl. Transl.)].
27. I. V. Komarov, M. Yu. Kornilov, A. V. Turov, N. A. Derevyanko, and A. A. Ishchenko, *Zhurn. Obshch. Khim.*, 1989, **59**, 2356 [*J. Gen. Chem. USSR*, 1989, **59** (Engl. Transl.)].
28. K. B. Simonsen, N. Svenstrup, J. Lau, O. Simonsen, P. Mork, G. J. Kristensen, and J. Becher, *Synthesis*, 1996, 407.
29. J. J. P. Stewart, *J. Computer-Aided*, 1990, **4**, 1.
30. V. E. Kampar, *Usp. Khim.*, 1982, **51**, 185 [*Russ. Chem. Rev.*, 1982, **51** (Engl. Transl.)].
31. N. A. Davidenko and A. A. Ishchenko, *Chem. Phys.*, 1999, **247**, 237.
32. N. A. Davidenko, A. A. Ishchenko, A. K. Kadashchuk, N. G. Kuvshinskii, N. I. Ostapenko, and Yu. A. Skryshevskii, *Fizika Tverdogo Tela*, 1999, **41**, 203 [*Phys. Sol. State*, 1999, **41** (Engl. Transl.)].

Received August 28, 2003;
in revised form February 2, 2004